Supplementary Information (SI) for Journal of Materials Chemistry C.

Supporting Information

Interlaced $NiCoO_2$ nanoparticle/nanosheet films for electrochromic energy storage devices with wide-band optical modulation and robust stability

Yongchao Liu,‡ Yu Zhong,‡ Huanhuan Liu, Pengyang Lei, Shiyou Liu, Jinhui Wang* and Guofa Cai*

Key Laboratory for Special Functional Materials of Ministry of Education, National & Local Joint Engineering Research Center for High-efficiency Display and Lighting Technology, School of Nanoscience and Materials Engineering, Henan University, Kaifeng 475004,

** Corresponding author: jinhui.wang@henu.edu.cn (Jinhui Wang); caiguofa@henu.edu.cn (Guofa Cai).*

‡ Yongchao Liu and Yu Zhong contributed equally to this work.

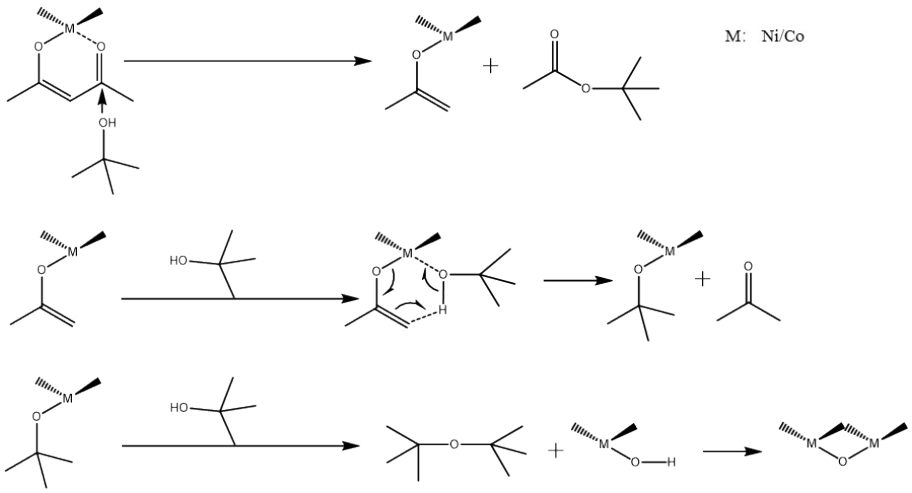

Fig. S1 Schematic diagram of the reaction process of $NiCoO_2$ using the solvothermal method.

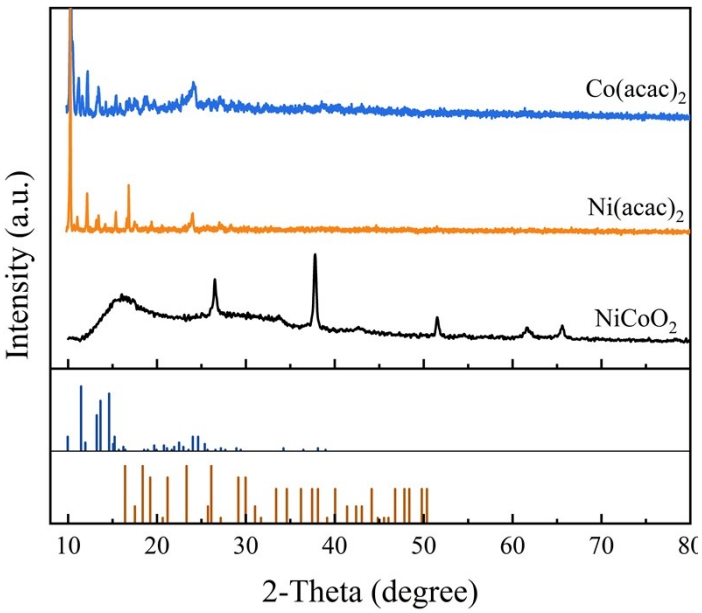

Fig. S2 XRD diffraction of $Ni(acac)_2$ and $Co(acac)_2$.

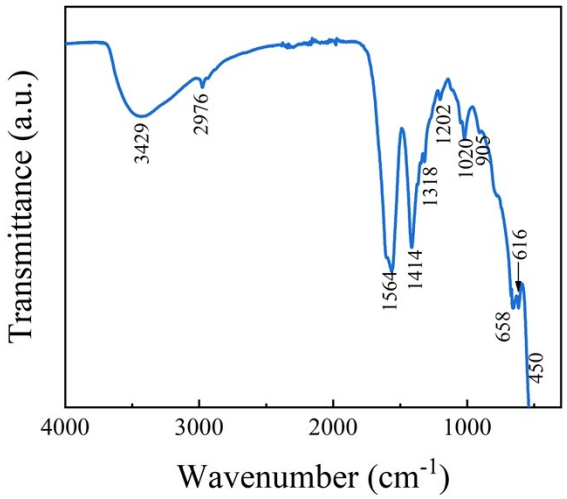

Fig. S3 FTIR spectra of the $NiCoO_2$ precipitate at the wavenumber of 400 to 4000 cm^{-1}.

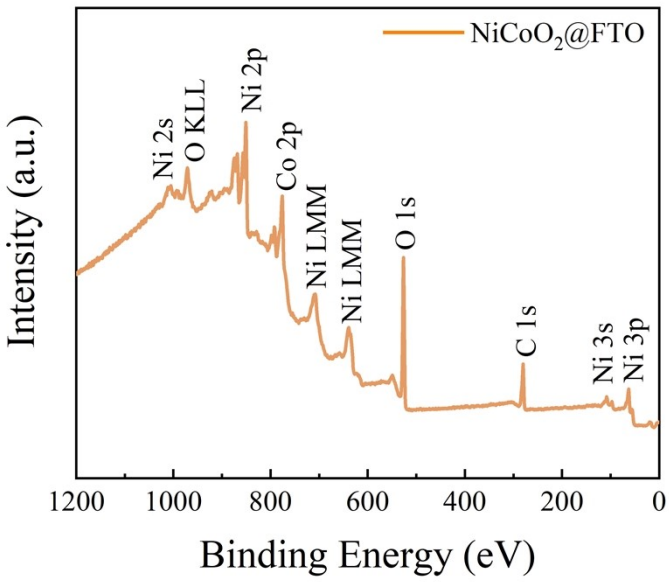

Fig. S4 The XPS full spectrum of the $NiCoO_2$ thin film grown on FTO substrates.

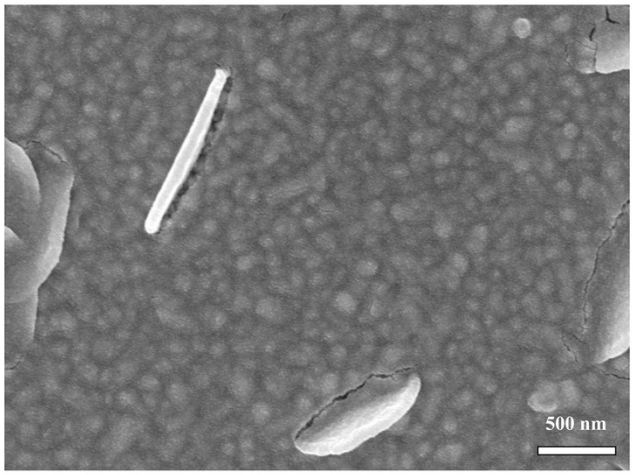

Fig. S5 SEM image of the $NiCoO_2$ thin film.

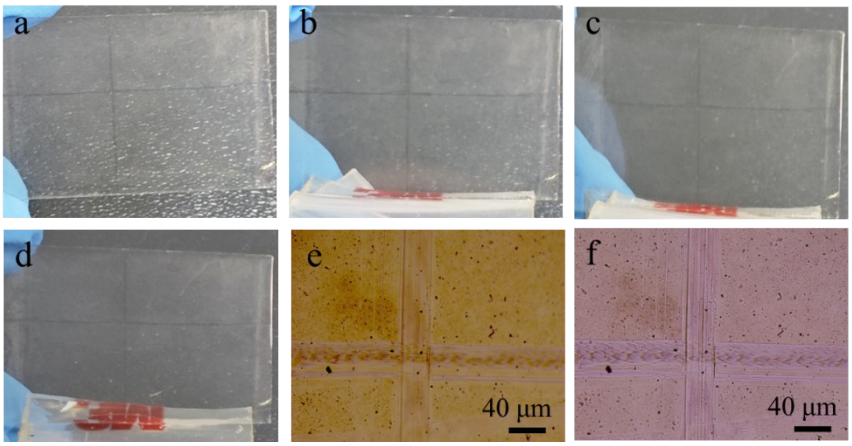

Fig. S6 Tape peeling test of the $NiCoO_2$ thin film: Digital photos of the film without peeling (a), peeling once (b), peeling twice (c), and peeling thrice (d), respectively; Optical microscope images of the $NiCoO_2$ thin film before (e) and after (f) tape peeling thrice.

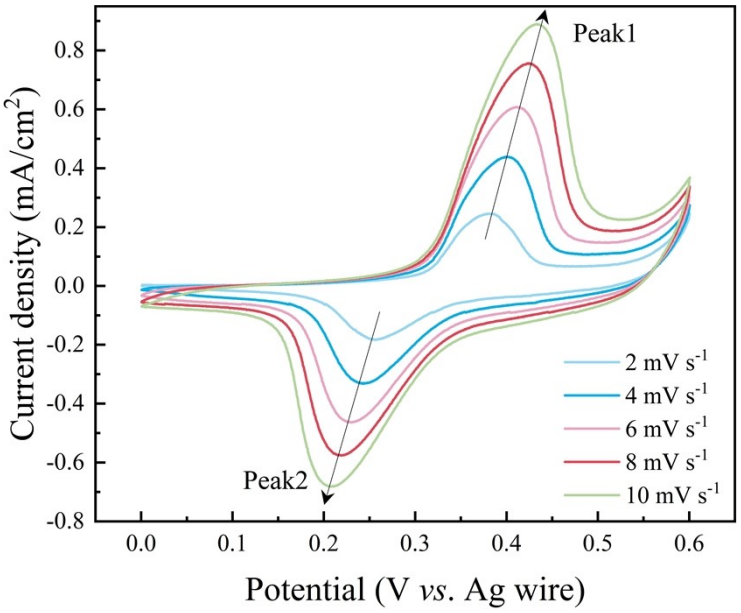

Fig. S7 CV curves of film at diferent scan rates from 2 to 10 mV s^{-1}.

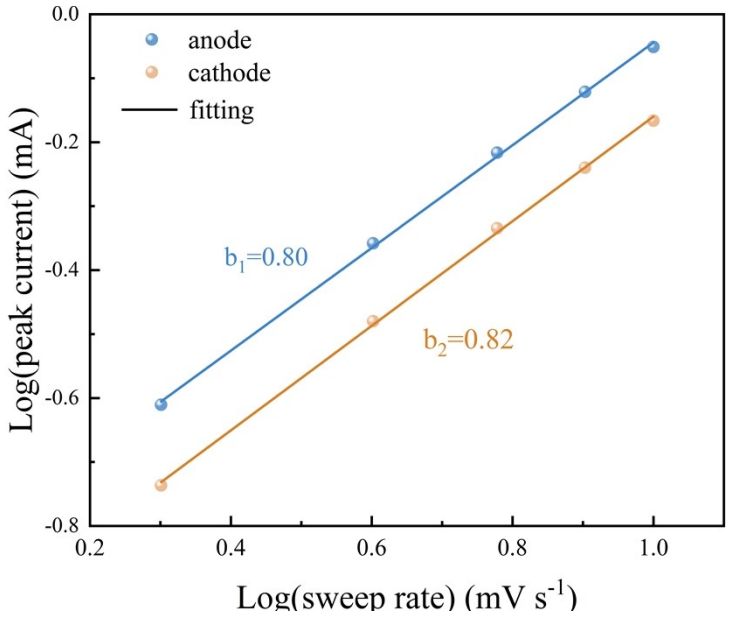

Fig. S8 Calculation of b value according to the relationship between log(*v*) and log(*i*).

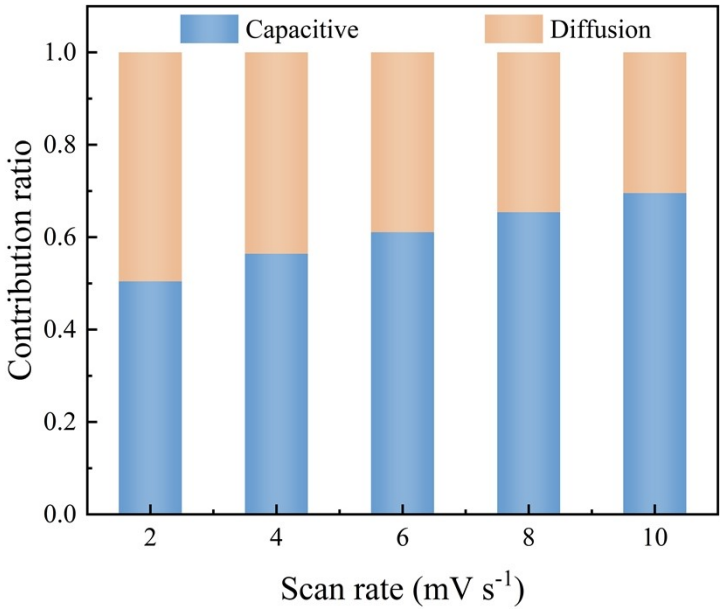

Fig. S9 Capacitive and diffusion contributions of the film at different scan rates.

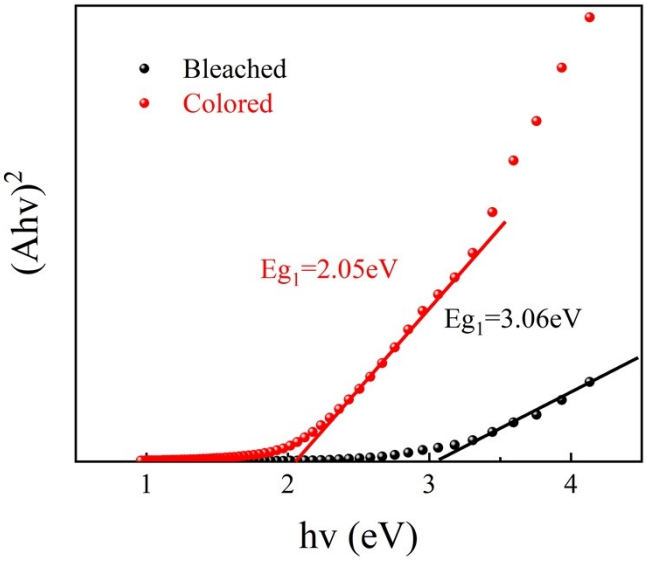

Fig. S10 The optical band gap of $NiCoO_2$ thin film in the colored and bleached states.

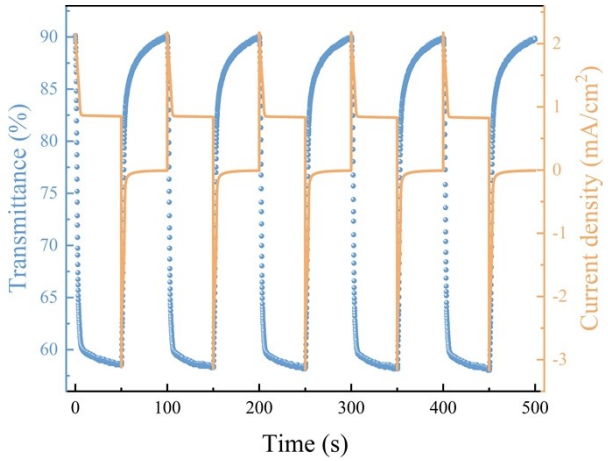

Fig. S11 Current response and in situ transmittance response spectra of the film at 900 nm by applying square wave potentials of -0.2 and 0.6 V.

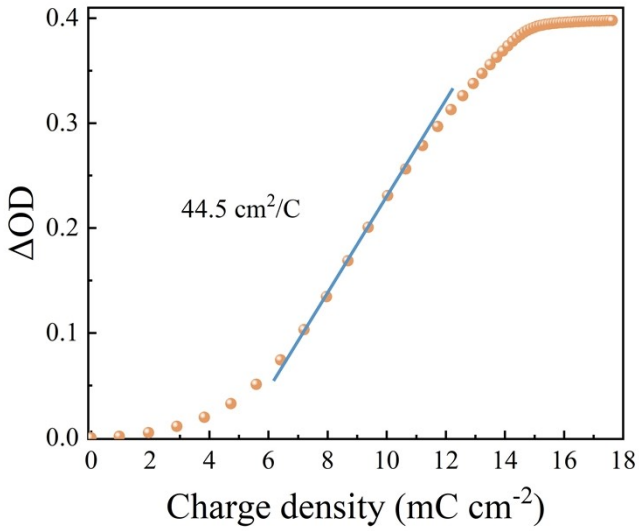

Fig. S12 Coloration efficiency of the $NiCoO_2$ thin film in 1 M KOH electrolyte at 550 nm.

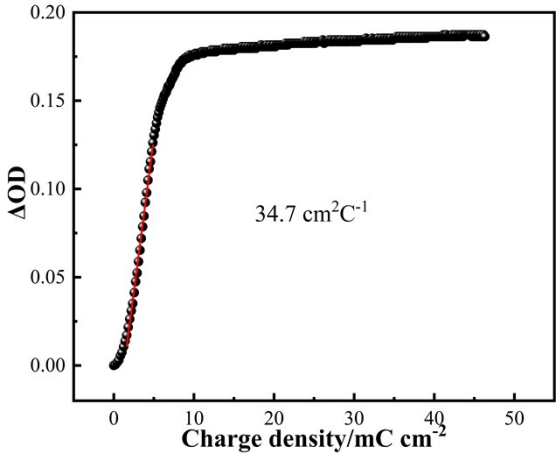

Fig. S13 Coloring efficiency of the film at 900 nm.

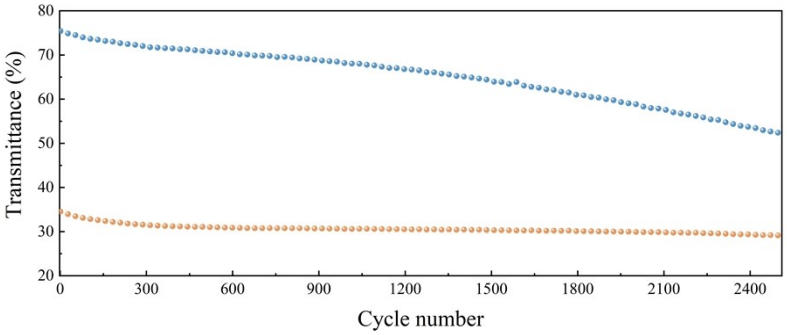

Fig. S14 Cycling stability of $NiCoO_2$ thin films in 1M KOH electrolyte for 2500 cycles at 550 nm.

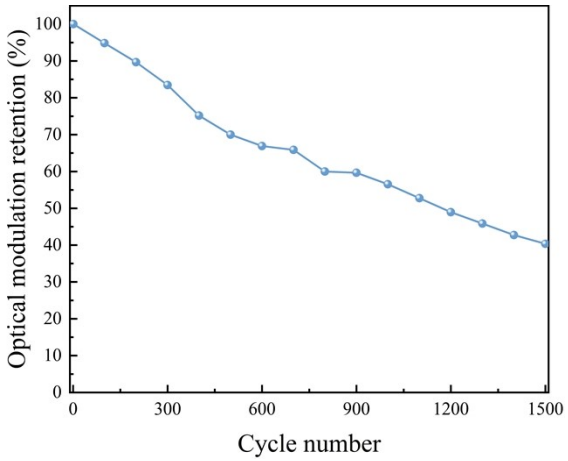

Fig. S15 Cycling stability of the films at 900 nm for 1500 cycles.

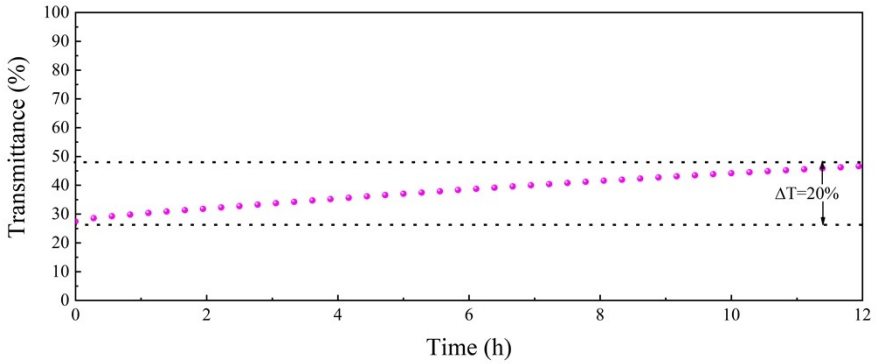

Fig. S16 Optical memory of $NiCoO_2$ thin films in the colored state at 550 nm under open-circuit potential.

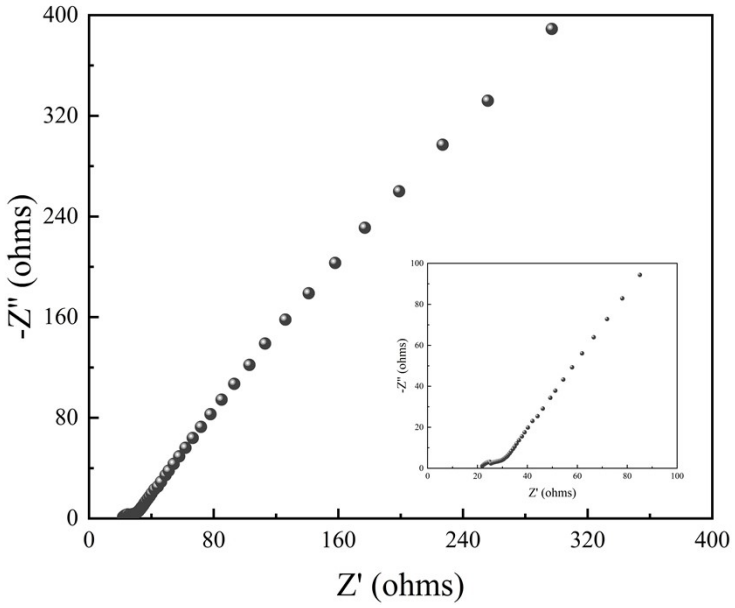

Fig. S17 Nyquist plots of the $NiCoO_2$ film.

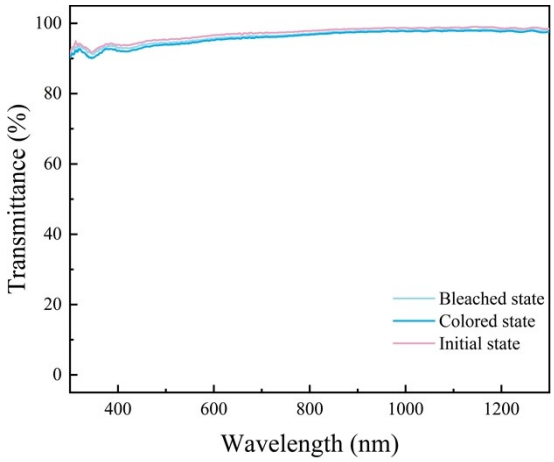

Fig. S18 Transmittance spectra of the rGO film in the bleached state (-0.8 V vs. Ag wire) and colored state (0.6 V vs. Ag wire) .

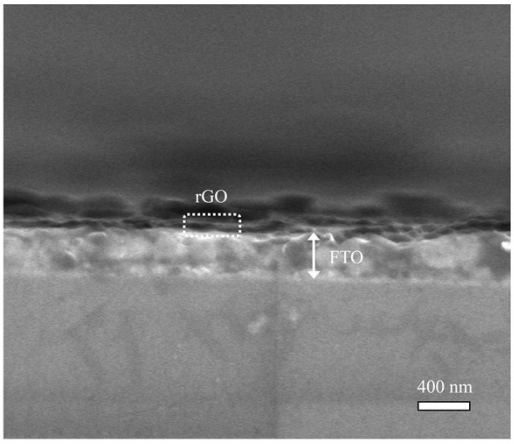

Fig. S19 Cross-sectional image of the rGO film on the FTO substrate.

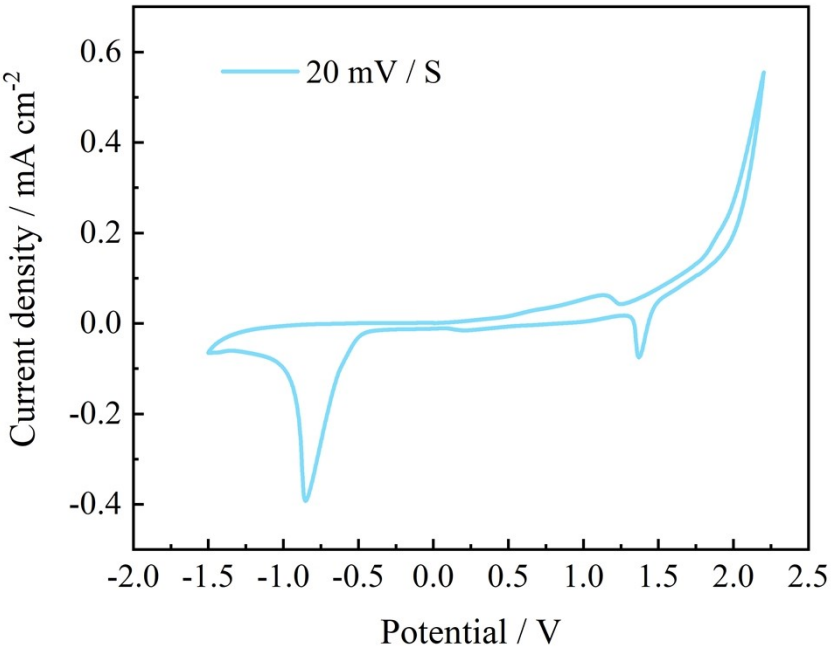

Fig. S20 CV curve of the electrochromic energy storage device at a scan rate of 20 mV/s.

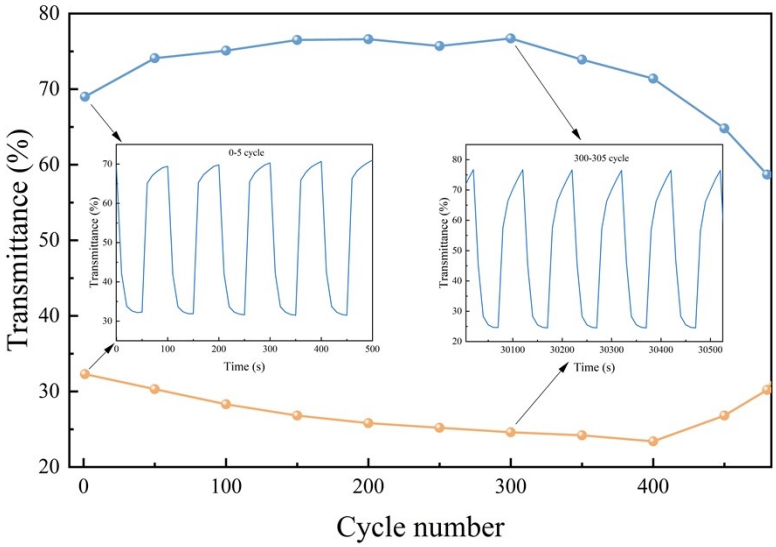

Fig. S21 Cycling stability of the device in 1M KOH over 480 cycles.

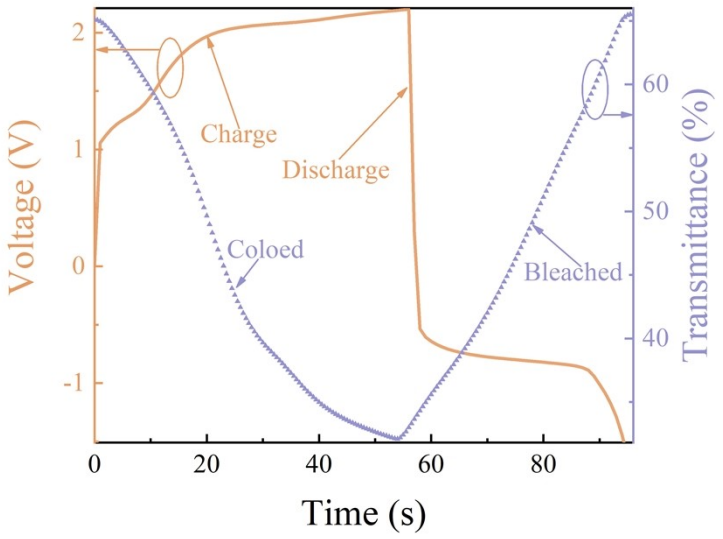

Fig. S22 GCD curve of the electrochromic energy storage device at a current density of 0.32 mA/cm^2, accompanied by in situ dynamic spectrum at 550 nm.

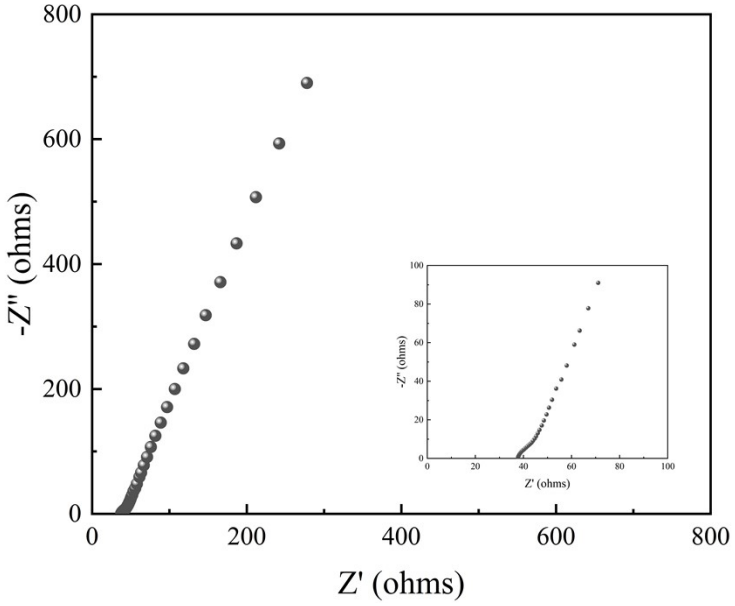

Fig. S23 Nyquist plots of the assembled EESD.

Fig. S24 Measured voltage of two devices in series in the colored state.

Table S1 Quantitative XPS analysis of $NiCoO_2$ thin films.

Name	Position	Area	FWHM	%At Conc
Ni 2p	851.00	56988.85	4.35	10.41
Co 2p	776.00	54765.59	6.01	11.27
C 1s	280.00	13429.41	3.60	35.69
O 1s	526.00	45011.66	3.79	42.63

Table S2 The fitting parameters of $NiCoO_2$ thin films.

Name	Ni^{2+}		Ni^{3+}		$Ni_{sat.1}$	$Ni_{sat.2}$	$Ni_{sat.3}$	$Ni_{sat.4}$	Co^{2+}		Co^{3+}		Co $_{sat.1}$	Co $_{sat.2}$
	2p1/2	2p3/2	2p1/2	2p3/2					2p1/2	2p3/2	2p1/2	2p3/2		
Position (eV)	867.8	849.9	869.3	851.6	856.9	874.8	861.2	878.0	797.0	781.2	795.3	779.6	784.5	802.1
Area	75764	151529	216170	432340	475261	290519	41584	40084	5262	9315	6247	10112	35920	16270
FWHM	2.1	1.5	3.2	2.6	4.5	5.4	3.3	3.9	2.5	2.6	2.3	2.0	9.8	7.1

Table S3 Quantitative analysis of $NiCoO_2$ thin films by elemental mapping.

Element	Ray type	Apparent concentration	K ratio	wt%	wt% Sigma	Atomic percentage
O	K-line system	2.03	0.00683	3.41	0.07	67.64
Si	K-line system	0.53	0.00418	0.59	0.01	6.69
Co	K-line system	0.30	0.00303	0.32	0.03	1.71
Ni	K-line system	0.34	0.00335	0.34	0.03	1.81
Sn	K-line system	7.30	0.07302	8.28	0.07	22.14

Table S4 The property comparison of the $NiCoO_2$ electrode with other reported works

Ref.	Materials	Optical modulation	Memory properties	Cyclic stability	Areal capacitance
This work	$NiCoO_2$	54.7% (550 nm) 34.8% (900 nm)	12 h (20%)	1500 (85%) 2500 (60%)	3.16 μAh/cm^2 (0.02 mA/cm^2)
Ref.[2]	NiO	37.8% (550 nm)	24 h (36%)	1000 (91%)	5.72×10^{-2} mAh/cm^2 (0.1 mA/cm^2)
Ref.[3]	$NiCoO_2$	64.2% (550 nm) 41.8% (1000 nm)	6.7 h (11.4%)	500 (75%)	33.6 mAh/g (0.25A/g)
Ref.[1]	NiO	30.0% (550 nm)	-	-	-
Ref.[4]	NiO	41.8% (650 nm)	-	10000 (86%)	2.08 F/cm^2 (1 mA/cm^2)
Ref. [5]	Co_3O_4	38% (633 nm)	-	-	-
Ref. [6]	Co_3O_4	13.9% (550 nm)	-	5 (100%)	99.67 F/g (0.5 A/g)
Ref. [7]	$NiCoO_2$	60% (550 nm)	0.8 h (32.6%)	1000 (62%)	194.5 mAh/cm^2 (0.04 mA/cm^2)
Ref.[8]	Co_3O_4/NiO	65.2% (600 nm)	-	300 (<90%)	-
Ref.[9]	$Co(OH)_2$/$Ni(OH)_2$	~20% (900 nm)	600 s (1%)	4000 (75%)	14.66 mF/cm^2 (0.2 mA/cm^2)
Ref.[10]	Ni_8-Co_2 oxide	49% (600 nm)	3000 s (10%)	1000 (49%)	-
Ref.[11]	Ni-Co oxide	55% (800 nm)	3000 s (<5%)	1000 (100%)	-

1. Dong, D.; Djaoued, H.; Vienneau, G.; Robichaud, J.; Brown, D.; Brüning, R.; Djaoued, Y., Electrochromic and colorimetric properties of anodic NiO thin films: Uncovering electrochromic mechanism of NiO. *Electrochimica Acta* **2020,** *335*, 135648.
2. Gao, Y.; Lei, P.; Zhang, S.; Liu, H.; Hu, C.; Kou, Z.; Wang, J.; Cai, G., A layer-stacked NiO nanowire/nanosheet homostructure for electrochromic smart windows with ultra-large optical modulation. *Nanoscale* **2023,** *15* (19), 8685-8692.
3. Lei, P.; Wang, J.; Zhang, P.; Liu, S.; Zhang, S.; Gao, Y.; Tu, J.; Cai, G., Growth of a porous $NiCoO_2$ nanowire network for transparent-to-brownish grey electrochromic smart windows with wide-band optical modulation. *Journal of Materials Chemistry C* **2021**.
4. Zhou, S.; Wang, S.; Zhou, S.; Xu, H.; Zhao, J.; Wang, J.; Li, Y., An electrochromic supercapacitor based on an MOF derived hierarchical-porous NiO film. *Nanoscale* **2020,** *12* (16), 8934-8941.
5. Ravi Dhas, C.; Venkatesh, R.; Sivakumar, R.; Dhandayuthapani, T.; Subramanian, B.; Sanjeeviraja, C.; Moses Ezhil Raj, A., Electrochromic performance of chromium-doped Co_3O_4 nanocrystalline thin films prepared by nebulizer spray technique. *J Alloy Compd* **2019,** *784*, 49-59.
6. He, Y.; Tao, X.; Li, Z.; Gao, G.; Zhuang, J.; He, L.; Li, Y.; Wang, Y.; Sun, D.; Xie, A., The Mg-Co_3O_4 coating on indium tin oxide film with improved electrochromic and energy storage properties by sol-gel spin coating. *Ceramics International* **2023,** *49* (19), 32237-32245.
7. Kou, Z.; Wang, J.; Tong, X.; Lei, P.; Gao, Y.; Zhang, S.; Cui, X.; Wu, S.; Cai, G., Multi-functional electrochromic energy storage smart window powered by CZTSSe solar cell for intelligent managing solar radiation of building. *Solar Energy Materials and Solar Cells* **2023,** *254*.
8. Zhao, H.; Meng, Y.; Yu, H.; Li, Z.; Liu, Z., 1D/2D Co_3O_4/NiO composite film for high electrochromic performance. *Ceramics International* **2022,** *48* (21), 32205-32212.
9. Lee, Y.-H.; Kang, J. S.; Park, J.-H.; Kang, J.; Jo, I.-R.; Sung, Y.-E.; Ahn, K.-S., Color-switchable electrochromic $Co(OH)_2$/$Ni(OH)_2$ nanofilms with ultrafast kinetics for multifunctional smart windows. *Nano Energy* **2020,** *72*, 104720.
10. Kim, K. H.; Morohoshi, M.; Abe, Y., Color modulation of electrochromic nanosheet-structured nickel-cobalt oxide thin films. *Applied Physics A* **2022,** *128* (6), 507.

11. Kim, K. H.; Numata, K.; Morohoshi, M.; Abe, Y., Morphological evolution of electrochromic nanosheet-structured nickel-cobalt oxide thin films. *Materials Letters* **2022,** *329*, 133192.